

# Role of Ambient Pressure on Colliding Jets

Minglei Li,<sup>1,2</sup> Abhishek Saha,<sup>2,3,\*</sup> Chao Sun,<sup>1</sup> and Chung K. Law<sup>2,1</sup>

<sup>1</sup>*Center for Combustion Energy, Tsinghua University, Beijing 100084, China*

<sup>2</sup>*Department of Mechanical and Aerospace Engineering,  
Princeton University, Princeton, NJ 08544, USA*

<sup>3</sup>*Department of Mechanical and Aerospace Engineering,  
University of California San Diego, La Jolla, CA 92093, USA*

(Dated: July 29, 2022)

The merging-vs-bouncing response of obliquely-oriented colliding jets under elevated and reduced gaseous environment pressures was experimentally examined. Results on water and n-tetradecane show that there exists a critical pressure below which increasing pressure promotes bouncing while beyond which merging is promoted instead, leading to a non-monotonic influence of pressure on the non-coalescence outcomes of collisional jets. This trend is explained on the bases of air entrainment and boundary layer development within the intervening gas layer between the impacting jet surfaces.

## I. INTRODUCTION

Collision of two liquid masses in gaseous environments is a frequently occurring event in many natural and industrial processes, for example in cloud and raindrop formation as well as spray and mixing processes within liquid-fueled combustors such as diesel and rocket engines [1–7]. It has been found that the colliding masses, such as droplet-droplet [8–11], droplet-film [12–14] and jet-jet [15, 16], could result in the non-coalescence and hence bouncing outcomes instead of merging as nominally expected. The cause for the non-coalescence response is the presence of the intervening gas layer between the impacting liquid masses, which can be as thin as tens to hundreds of nanometers [17–20] and needs to be “squeezed” out by the impacting liquid surfaces before the impact momentum is dissipated. In particular, it has been conclusively demonstrated, for both the droplet and jet systems, that with increasing impact inertia, the collision response can evolve from merging, to bouncing, to merging again, and finally to merging followed by disintegration of the merged mass. For conceptual visualization, Fig. 1 shows the experimental images obtained in the course of the present investigation, for the suite of possible jet collision outcomes of soft merging (I), bouncing (II), and hard merging (III), with increasing impact inertia. Further increase in impact inertia beyond III leads to instabilities which disintegrate the collided jet structure. Such instabilities and the ensuing atomization have been extensively detailed in refs. [21, 22].

Recognizing the relevance of system pressure in automotive, airplane and rocket engines, studies on droplet-droplet collision have also demonstrated that increasing pressure promotes bouncing because of the increased pressure- and hence density-dependent interfacial mass that needs to be displaced. Furthermore, because of the substantial differences in the physical properties between water and hydrocarbons, with water having a larger sur-

face tension and stronger van der Waals force than alkanes, it was also shown that water droplets do not exhibit bouncing at atmospheric pressure, but they readily bounce at higher pressures. On the other hand, while hydrocarbon droplets bounce at atmospheric pressure, they merge at reduced pressures [9]. This property-dependent understanding is enlightening in that extensive investigations on hydrocarbon fuel spray processes for engine applications have inadvertently assumed droplet merging upon collision based on the results of water droplet collision at atmospheric pressure [23], and as such have led to biased spray statistics in analyzing engine combustion behavior.

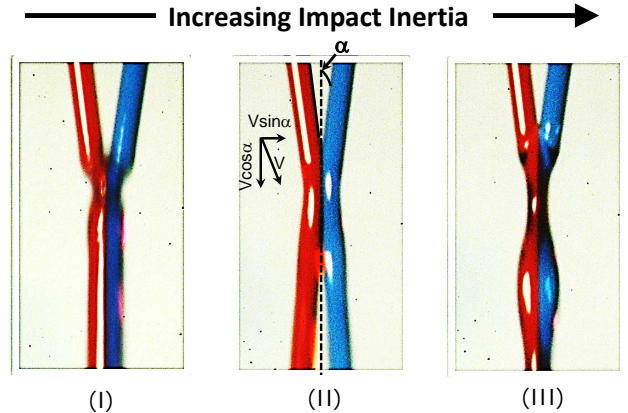


FIG. 1. Images showing the suite of the collision response with increasing collision velocity (or impact inertia). (I): soft merging; (II): bouncing; (III): hard merging. Liquid: dyed n-tetradecane; pressure: 1 bar.

In view of the above considerations, we have performed a systematic experimental investigation on obliquely oriented colliding jets under both elevated- and reduced-pressure environments. We shall show in due course the resistance to bouncing for water jets as versus hydrocarbon jets as observed for the droplet collision. Furthermore, we have also identified a new phenomenon that,

\* Email: asaha@eng.ucsd.edu

due to the development of boundary layer over the impacting air-jet interfaces, merging instead of bouncing can be promoted at higher pressures, which is contrary to the results of droplet collision.

The experimental arrangement, results, and analysis are sequentially presented in the following.

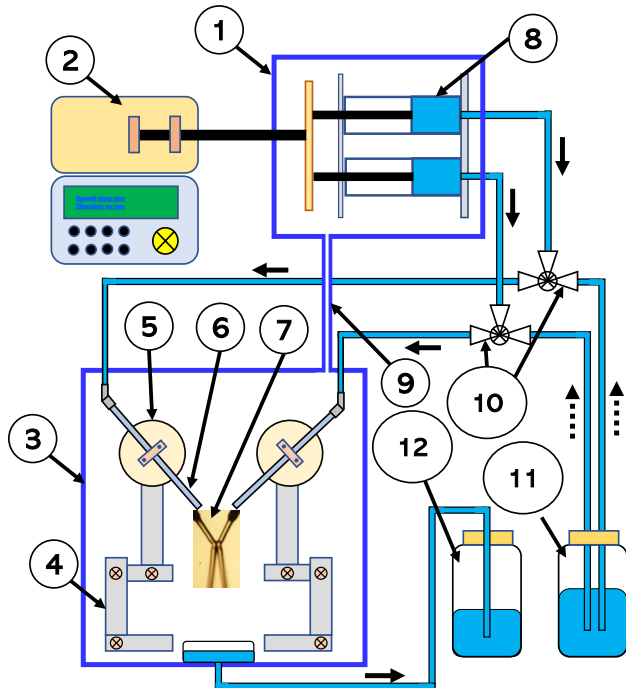


FIG. 2. Schematic illustration of the experimental apparatus. 1. Syringe chamber; 2. Syringe pump controller; 3. Jet chamber; 4. XYZ-micro-position stage; 5. Micro-rotation stage; 6. Jet nozzle; 7. Quartz observation window; 8. Glass syringes; 9. Pressure balance connector; 10. Three-way valves; 11. Liquid reservoir; 12. Waste liquid reservoir.

## II. EXPERIMENTS

Schematic of the experimental setup for the controlled-pressure jet collision experiments is shown in Fig. 2. To achieve ambient pressure control of the jets, two identical nozzles, together with their relative position and orientation manipulation system, are placed in a sealed chamber with five observation windows in three directions. A connected dual-chamber design keeps the pressure balance between the syringe chamber and the jet chamber, so that the stability of the fluid flux generated from the pump can be guaranteed under different pressure conditions. With this setup, the test liquid is first drawn into the glass syringes from a liquid reservoir, and then is injected to the nozzles inside the jet chamber to form colliding jets after the chamber pressure is established. The flow rate of the system can be varied from 1.0 to 28.0 ml/min with an accuracy of

$\pm 0.5\%$ . Considering the extra pressure resistance from the pipes, adapters and nozzles, the flux is calibrated under various pressure conditions, according to which the experimental results are further amended to keep the data accurate. Two identical nozzles with inner diameter of 200  $\mu\text{m}$  were designed by fixing the short thin-wall capillary tube inside a drilled copper column. Compared with the normally used glass capillary or needles, such nozzles yield sharper edges to avoid tip adhesive attraction of the liquid without increasing the pressure resistance, and hence is able to generate fluid jet with a larger velocity range. The angle and position of the nozzles are precisely manipulated through micro-rotation and XYZ-micro-positioning, which can be conveniently controlled outside the chamber through soft driver connectors. Technical grade de-ionized water and n-alkanes, specifically n-decane, n-dodecane, n-tetradecane and n-hexadecane, are used as the working fluids; their properties are listed in Table I. The bouncing-merging transition experiments at 1 bar (atmospheric) condition were performed on all the alkanes, while for experiments at elevated and reduced pressure, water and n-tetradecane were selected.

TABLE I. Properties of the liquids used for the study

Liquid	$\rho$ (kg/m <sup>3</sup> )	$\eta$ (10 <sup>-3</sup> Pa-s)	$\sigma$ (10 <sup>-3</sup> N/m)
Water	1000	1.01	72.90
n-Decane	730	0.92	23.83
n-Dodecane	750	1.34	25.35
n-Tetradecane	760	2.30	26.56
n-Hexadecane	773	3.00	27.47

## III. RESULTS AND DISCUSSION

The bouncing behavior of n-alkanes under the normal pressure (1 bar) condition are first investigated. By gradually varying the jet velocity and impact angle, we have mapped the regimes within which the collision yields (soft) merging, bouncing, and (hard) merging outcomes. Take n-tetradecane as an example. Figure 3a maps the collision merging-vs-bouncing response, and shows the dependence of critical velocity delineating the transition with the collisional angle of the jets. The critical velocities generate two boundaries, for hard and soft transitions, splitting the outcome into regimes I, II and III. It is seen that the soft merging transition boundary is nearly insensitive to  $\alpha$ , having an almost constant critical velocity, while the hard merging transition boundary has a strong dependence on the impact angle, with significant decreasing critical velocity. The two transition boundaries merge at a certain angle ( $\alpha_{cr}$ ), 38° for n-tetradecane, beyond which bouncing is not observed. Similar transition boundaries are obtained for n-hexadecane, n-dodecane and n-decane, with  $\alpha_{cr}$  be-

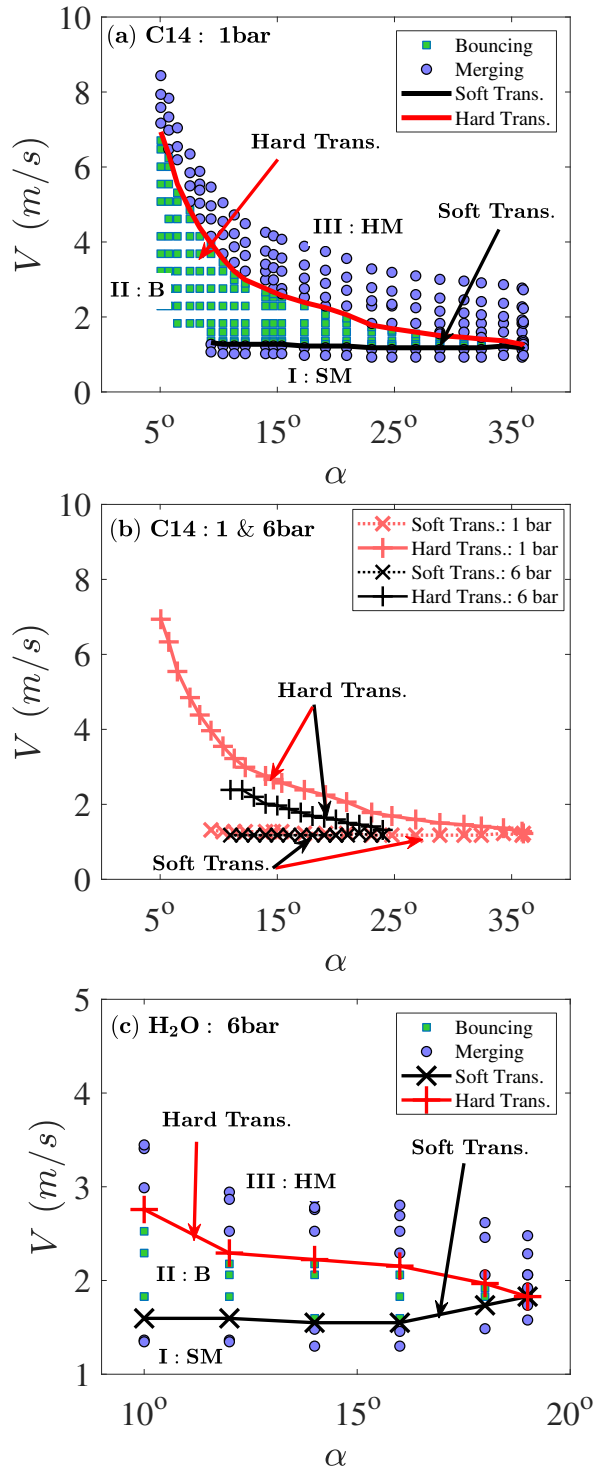


FIG. 3. (a) Regime map for n-tetradecane (C14) at 1 bar. (b) Comparison of regime boundaries for n-tetradecane (C14) at 1 bar and 6 bar. (c) Regime map for water (H<sub>2</sub>O) at 6 bar. Various impact outcomes: bouncing, (soft and hard) merging, and the (Hard and Soft) transition boundaries are shown. The data for n-tetradecane at 1 bar was presented in [16]. The uncertainty in  $V$  is about  $\pm 5\%$ . **SM**: Soft Merging; **B**: Bouncing; **HM**: Hard Bouncing.

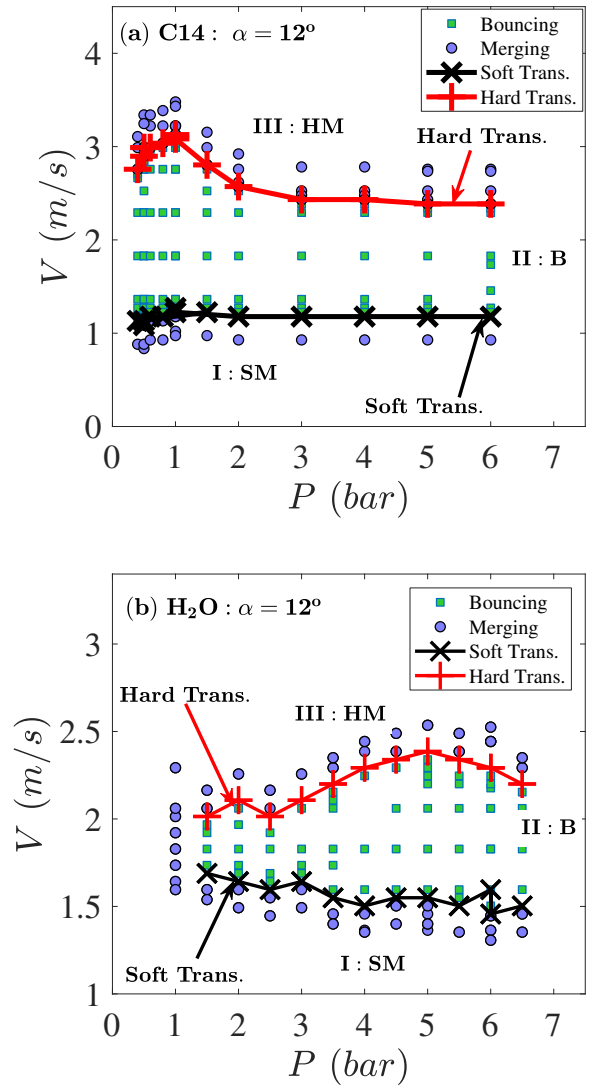


FIG. 4. Regime map as functions of the impact velocity and ambient pressure for: (a) n-tetradecane (C14) and (b) Water (H<sub>2</sub>O). Impact angle,  $\alpha=12^\circ$ . The uncertainty in  $V$  is about  $\pm 5\%$ . **SM**: Soft Merging; **B**: Bouncing; **HM**: Hard Bouncing.

ing  $44^\circ$ ,  $28^\circ$  and  $19^\circ$  respectively, as reported in our previous work [16]. In that work, we discussed and analyzed that the hard transition boundary is dominated by the gas-layer thickness ( $H_d$ ) evolution which scales as  $H_d/R = A_I St^{-2/3}$ , where  $St = (\rho_l RU)/\eta_g$  is the Stokes number,  $A_I$  a prefactor,  $\rho_l$  the liquid density,  $R$  the jet radius,  $\eta_g$  the air viscosity and  $U$  the effective impact velocity which is  $V \sin \alpha$  in the present case. The soft transition boundary is dominated by the Plateau-Rayleigh instability of the jet surface, leading to the velocity ratio,  $\Gamma = V/V_c$ , where  $V_c$  is the velocity of the capillary waves travelling along the jet.

Since the gas density can directly influence the inertia of the gas layer, it is straightforward to consider its effects by varying the gas pressure. First, to assess whether the pressure variation can affect the liquid side of the bounc-

ing jet, we captured the jet shape and measured the characteristic geometry parameters, including the contact length, maximum deformation and separation angle of the bouncing jets respectively under ambient pressures from 1 to 6 bar. Results show that the shape evolution of the liquid jets has no visible dependence on the system pressure, which implies that in this case the ambient pressure variation has no effect on the liquid side during the jet bouncing process. This is to be expected because the viscosity and surface tension of the liquid barely change within this pressure range, and the density ratio between liquid and air,  $\rho_l/\rho_g$ , is over 500, which is much larger than the gas density variation. Consequently, the influence of pressure on the non-coalescence behavior of the jets could only play a role through gas layer dynamics.

Subsequent extensive experimental investigation on jet collision in elevated and reduced pressure ambience were conducted, showing that, similar to droplet collision, no bouncing is observed for water jets under normal pressure, and is exhibited at higher pressures, such as 6 bar as shown in Fig. 3c. For n-tetradecane jets, bouncing is observed at normal pressure, but is suppressed when the pressure is reduced to 0.2 bar.

The investigation, however, identified an important qualitative difference between droplet and jet collisions at high pressures. That is, with increasing impact inertia and within the range of higher pressures investigated, the hard transition boundary, from bouncing to hard merging, is reduced instead of expanded. As shown in Fig. 3b, the hard transition velocities at 6 bar are much smaller than those at 1 bar, leading to a narrower bouncing regime and rendering the critical collisional angle decreasing from  $38^\circ$  to  $24^\circ$ .

To further explore and quantify this new phenomenon, additional experiments were conducted with water and n-tetradecane for various pressures, while keeping the jet collision angle fixed. Figure 4 quantifies the non-monotonicity of the hard transition boundary with increasing pressure: first increasing and then decreasing, and hence promoting and inhibiting bouncing respectively. The transition state occurs at a critical pressure  $P_{cr}$  of 0.9 bar for n-tetradecane (Fig. 4a) and 5 bar for water (Fig. 4b).

To identify the cause of this non-monotonic response, that the bouncing jets can keep stable is that the intervening gas layer between the liquid interfaces is continuously being supplemented by upstream air entrainment, which is the major difference from droplet collision. Since the increasing pressure cannot influence the liquid deformation, as mentioned earlier, further analysis shows that increasing ambient pressure can also reduce the extent of the gas entrainment by reducing the air boundary layer thickness. Specifically, in analogy with the boundary layer flow over a plate, the air boundary layer thickness over the jet surface would scale as  $\delta \sim l/Re^{1/2}$ , where  $Re = \rho_g V l / \eta_g$  is the jet Reynolds number,  $l$  the free jet length, and  $\rho_g$  and  $\eta_g$  the gas density and viscosity coefficient respectively. Since  $\rho_g$  increases with pressure, while  $\eta_g$  is insensitive to it,  $\delta$  will decrease with increasing pressure. This reduced boundary layer thickness not only counteracts the increased mass entrainment due to the increased pressure, but it also reduces the interfacial separation distance and hence promotes the attractive van der Waals force. Consequently, the observed non-monotonic trend is due to the joint influence of pressure variation on gas layer properties, gas density and entrainment. The coalescence-vs-bouncing responses of droplet-droplet and jet-jet collision can therefore be interpreted from a unified viewpoint.

#### IV. SUMMARY

We have conclusively identified the pressure effect on the jet-jet collision response. Unlike the widely investigated droplet-droplet collision case, pressurized ambient gas ambient does not always promote bouncing in jet collision. A unified non-monotonic trend of bouncing transition boundary is identified, leading to a critical pressure under which the collisional jets achieve maximum bouncing. Understanding gained herein yields a useful reference for practical applications, offering an additional consideration to the role of pressure on the bouncing versus coalescence of colliding jets.

- 
- [1] W. Macklin and P. Hobbs, Subsurface phenomena and the splashing of drops on shallow liquids, *Science* **166**, 107 (1969).
  - [2] B. Ching, M. W. Golay, and T. J. Johnson, Droplet impacts upon liquid surfaces, *Science* **226**, 535 (1984).
  - [3] G. Falkovich, A. Fouxon, and M. Stepanov, Acceleration of rain initiation by cloud turbulence, *Nature* **419**, 151 (2002).
  - [4] I. V. Roisman and C. Tropea, Impact of a drop onto a wetted wall: description of crown formation and propagation, *J. Fluid Mech.* **472**, 373 (2002).
  - [5] W. Bouwhuis, R. C. van der Veen, T. Tran, D. L. Keij, K. G. Winkels, I. R. Peters, D. van der Meer, C. Sun, J. H. Snoeijer, and D. Lohse, Maximal air bubble entrainment at liquid-drop impact, *Phys. Rev. Lett.* **109**, 264501 (2012).
  - [6] T. Tran, H. de Maleprade, C. Sun, and D. Lohse, Air entrainment during impact of droplets on liquid surfaces, *J. Fluid Mech.* **726** (2013).
  - [7] A. Saha, Y. Wei, X. Tang, and C. K. Law, Kinematics of vortex ring generated by a drop upon impacting a liquid pool, *J. Fluid Mech.* **875**, 842 (2019).

- [8] Y. Jiang, A. Umemura, and C. Law, An experimental investigation on the collision behaviour of hydrocarbon droplets, *J. Fluid Mech.* **234**, 171 (1992).
- [9] J. Qian and C. K. Law, Regimes of coalescence and separation in droplet collision, *J. Fluid Mech.* **331**, 59 (1997).
- [10] P. Zhang and C. K. Law, An analysis of head-on droplet collision with large deformation in gaseous medium, *Phys. Fluids* **23**, 042102 (2011).
- [11] C. Tang, J. Zhao, P. Zhang, C. K. Law, and Z. Huang, Dynamics of internal jets in the merging of two droplets of unequal sizes, *J. Fluid Mech.* **795**, 671 (2016).
- [12] K. L. Pan and C. K. Law, Dynamics of droplet–film collision, *J. Fluid Mech.* **587**, 1–22 (2007).
- [13] X. Tang, A. Saha, C. K. Law, and C. Sun, Nonmonotonic response of drop impacting on liquid film: mechanism and scaling, *Soft Matter* **12**, 4521 (2016).
- [14] X. Tang, A. Saha, C. K. Law, and C. Sun, Bouncing-to-merging transition in drop impact on liquid film: Role of liquid viscosity, *Langmuir* **34**, 2654 (2018).
- [15] N. Wadhwa, P. Vlachos, and S. Jung, Noncoalescence in the oblique collision of fluid jets, *Phys. Rev. Lett.* **110**, 124502 (2013).
- [16] M. Li, A. Saha, D. Zhu, C. Sun, and C. K. Law, Dynamics of bouncing-versus-merging response in jet collision, *Phys. Rev. E* **92**, 023024 (2015).
- [17] G. P. Neitzel and P. Dell’Aversana, Noncoalescence and nonwetting behavior of liquids, *Ann. Rev. Fluid Mech.* **34**, 267 (2002).
- [18] Y. Couder, E. Fort, C.-H. Gautier, and A. Boudaoud, From bouncing to floating: noncoalescence of drops on a fluid bath, *Phys. Rev. Lett.* **94**, 177801 (2005).
- [19] S. T. Thoroddsen, M.-J. Thoraval, K. Takehara, and T. Etoh, Micro-bubble morphologies following drop impacts onto a pool surface, *J. Fluid Mech.* **708**, 469 (2012).
- [20] X. Tang, A. Saha, C. K. Law, and C. Sun, Bouncing drop on liquid film: Dynamics of interfacial gas layer, *Phys. Fluids* **31**, 013304 (2019).
- [21] J. W. Bush and A. E. Hasha, On the collision of laminar jets: fluid chains and fishbones, *J. Fluid Mech.* **511**, 285 (2004).
- [22] N. Bremond and E. Villermaux, Atomization by jet impact, *J. Fluid Mech.* **549**, 273 (2006).
- [23] P. O’Rourke and F. Bracco, Modeling of droplet interactions in thick sprays and a comparison with experiments: Startified Charge Auto. Eng. Conf., 101–115, *Inst. Mech. Eng. Pub. ISMB 0-85298-4693*.